University of Groningen

Hydrogenation of PAH cations

Boschman, L.; Reitsma, G.; Cazaux, S.; Schlathölter, Thomas; Hoekstra, R.; Spaans, M.; Gonzalez Magana, Olmo

IMPORTANT NOTE: You are advised to consult the publisher's version (publisher's PDF) if you wish to cite from it. Please check the document version below.

Document Version
Publisher's PDF, also known as Version of record

[Link to publication in University of Groningen/UMCG research database](#)

HYDROGENATION OF PAH CATIONS: A FIRST STEP TOWARD H₂ FORMATION

L. Boschman[1,2], G. Reitsma[2], S. Cazaux[1], T. Schlathölter[2], R. Hoekstra[2], M. Spaans[1], and O. González-Magaña[2]

[1] Kapteyn Astronomical Institute, University of Groningen, P.O. Box 800, 9700 AV Groningen, The Netherlands; boschman@astro.rug.nl
[2] KVI Atomic and Molecular Physics, University of Groningen, Zernikelaan 25, 9747 AA Groningen, The Netherlands

ABSTRACT

Molecular hydrogen is the most abundant molecule in the universe. A large fraction of H₂ forms by association of hydrogen atoms adsorbed on polycyclic aromatic hydrocarbons (PAHs), where formation rates depend crucially on the H sticking probability. We have experimentally studied PAH hydrogenation by exposing coronene cations, confined in a radio-frequency ion trap, to gas phase atomic hydrogen. A systematic increase of the number of H atoms adsorbed on the coronene with the time of exposure is observed. Odd coronene hydrogenation states dominate the mass spectrum up to 11 H atoms attached. This indicates the presence of a barrier preventing H attachment to these molecular systems. For the second and fourth hydrogenations, barrier heights of 72 ± 6 meV and 40 ± 10 meV, respectively, are found, which are in good agreement with theoretical predictions for the hydrogenation of neutral PAHs. Our experiments, however, prove that the barrier does not vanish for higher hydrogenation states. These results imply that PAH cations, as their neutral counterparts, exist in highly hydrogenated forms in the interstellar medium. Due to this catalytic activity, PAH cations and neutrals seem to contribute similarly to the formation of H₂.

Key words: astrochemistry – ISM: molecules

Online-only material: color figures

1. INTRODUCTION

Molecular hydrogen is the most abundant molecule in the universe and the main constituent of regions where stars are forming. H₂ plays an important role in the chemistry of the interstellar medium (ISM), and its formation governs the transformation of atomic diffuse clouds into molecular clouds. Because of the inefficient gas phase routes to form H₂, dust grains have been recognized to be the favored habitat to form H₂ molecules (Oort & van de Hulst 1946; Gould & Salpeter 1963). The sticking of H atoms onto surfaces has received considerable attention because this mechanism governs the formation of H₂, but also other molecules that contain H atoms. The sticking of H atoms onto dust grains can also be an important mechanism to cool interstellar gas (Spaans & Silk 2000). In the past few decades, a plethora of laboratory experiments and theoretical models have been developed to understand how H₂ forms. As H atoms arrive on dust surfaces, they can be weakly (physisorbed) or strongly (chemisorbed) bound to the surface. The sticking of H in the physisorbed state (Pirronello et al. 1997, 1999, 2000; Perry & Price 2003) and in the chemisorbed state (Zecho et al. 2002; Hornekær et al. 2006; Mennella 2006) has been highlighted by several experiments on different types of surfaces (amorphous carbon, silicates, and graphite).

In the ISM, dust grains are mainly carbonaceous or silicate particles with various sizes and represent an important surface for the formation of H₂. However, a large part (~50%) of the available surface area for chemistry is in the form of very small grains or polycyclic aromatic hydrocarbons (PAHs; Weingartner & Draine 2001). These PAHs are predicted to have characteristics similar to graphite surfaces; however, once the first H atom is chemisorbed on the basal plane, subsequent adsorptions of H atoms in pairs appear to be barrierless for the para dimer and with a reduced barrier for the ortho dimer (Rougeau et al. 2006). H₂ can then form by involving a pre-adsorbed H atom in monomer (Sha & Jackson 2002; Morisset

et al. 2003, 2004; Martinazzo & Tantardini 2006) or in a para-dimer configuration (Bachellerie et al. 2007). However, while these routes represent efficient paths to form H₂, the inefficient sticking of H atoms in monomers constitutes an important obstacle to enter the catalytic regime for H₂ formation. This results in a very low H₂ formation efficiency on graphitic/PAH surfaces (Cazaux et al. 2011).

The hydrogenation on the PAH edges has been identified as an important route to form H₂ in the ISM (Bauschlicher 1998; Hirama et al. 2004; Le Page et al. 2009; Mennella et al. 2012; Thrower et al. 2012). Density functional theory calculations have shown that the first hydrogenation of neutral coronene is associated with a barrier (~60 meV) but that subsequent hydrogenation barriers vanish (Rauls & Hornekær 2008). Recently, coronene films exposed to H/D atoms at high temperature were studied by means of IR spectroscopy (Mennella et al. 2012) and mass spectrometry (Thrower et al. 2012). These measurements showed that neutral PAHs, when highly hydrogenated, are efficient catalysts for the formation of H₂, and confirmed the high H₂ formation rate attributed to PAHs in photodissociation regions (PDRs; Mennella et al. 2012).

PAH cations, which are usually present at lower extinction A_V, and therefore reside at the surfaces of PDRs, also represent an important route to form H₂ (Bauschlicher 1998; Le Page et al. 2009). The addition of the first H atom is predicted to be barrierless. This reaction is exothermic but the product should be stabilized by IR emission. A second H atom can react with the already adsorbed H to form H₂ without a barrier (Bauschlicher 1998; Hirama et al. 2004).

In this Letter, we study experimentally the hydrogenation of coronene cations in the gas phase through exposure to hydrogen atoms. By using mass spectrometry, we show that odd hydrogenation states of coronene cations predominantly populate the mass spectrum. Our results highlight the fact that the further hydrogenation of PAH cations is associated with a barrier if the number already attached H atoms is odd, and no
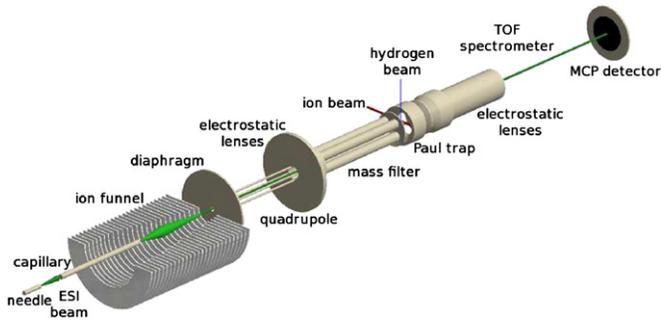
Figure 1. Setup used, with the ion funnel, quadrupoles, ion trap, hydrogen source, and detector.

(A color version of this figure is available in the online journal.)

barrier if this number is even. This alternating barrier–no-barrier occurrence seems to remain with increasing hydrogenation. These results suggest that PAH cations can also enjoy highly hydrogenated states in the ISM, and acts as catalysts for H_2 formation.

2. EXPERIMENTS

In this pilot experiment, we show the feasibility of studying the hydrogenation of PAHs in the gas phase. For this purpose, we use a setup designed to study molecular ions in a radio-frequency (RF) ion trap. Time-of-flight (TOF) mass spectrometry of the trap content is used to identify the changes in mass of the coronene cations and therefore deduce their respective degrees of hydrogenation.

2.1. Setup

The experiments have been performed using a home-built tandem-mass spectrometer shown schematically in Figure 1 (Bari et al. 2011). A beam of singly charged coronene radical cations ($[C_{24}H_{12}]^+$, m/z 300) was extracted from an electrospray ion source. The ions were phase-space compressed in an RF ion funnel and subsequently in an RF quadrupole ion guide. Mass selection was accomplished by using an RF quadrupole mass filter. Accumulation of the ions took place in a three-dimensional RF ion trap (Paul trap). An He buffer gas at room temperature was used to collisionally cool the trapped cations. Exposure to gas-phase atomic hydrogen for variable periods of time led to multiple hydrogen adsorption on the coronene cations. An electric extraction field was then applied between the trap end caps to extract the trapped hydrogenated cations into a TOF mass spectrometer with a resolution of $M/\Delta M \sim 200$. To obtain mass spectra of sufficient statistics, typically a couple of hundred TOF traces were accumulated.

Electrospray ionization allows us to gently transfer ions from the liquid phase into the gas phase. Inspired by the method of Maziarz (2005), we have run the ion source with a solution consisting of $600 \, \mu L$ of saturated solution of coronene in methanol, $350 \, \mu L$ of HPLC grade methanol, and $50 \, \mu L$ of 10 mM solution of $AgNO_3$ solution in methanol. In the liquid phase, electron transfer from a coronene molecule to a silver ion leads to formation of the required radical cation.

The trapped ions are exposed to hydrogen atoms produced from H_2 by a Slevin type source which has been extensively used in crossed beam experiments (Hoekstra et al. 1991; Bliek et al. 1997). While in the earlier work the dissociation fractions were determined by means of electron impact excitation or He II line emission, we now use charge removal (captured ionization)

and dissociation induced by 40 keV He^{2+}. For these processes, the cross sections are well known (Shah & Gilbody 1978). In this way, we determine a hydrogen dissociation fraction of $n(H)/(n(H)+n(H_2)) \approx 0.3$. The temperature of the H beam is around room temperature ($\sim$25 meV).

2.2. Results

Coronene ions are exposed to a constant flux of H atoms for different periods of time before their degree of hydrogenation is determined by means of mass spectrometry. The irradiation time is varied from 1.0 up to 30 s to study the time dependence of coronene hydrogenation.

The data obtained from our experiment are a series of mass spectra of hydrogenated coronene cations as a function of H exposure time. Some of the spectra are shown in Figure 2. Figure 2(a) shows the mass spectrum of the native $m/z = 300$ coronene cations. A similar, thus unchanged, mass spectrum is obtained (not shown in this article) if we irradiate coronene cations with molecular hydrogen. This means that molecular hydrogen does not stick to coronene cations at room temperature.

After turning on the hydrogen source and exposing the coronene cations to the atomic hydrogen beam for 1.0 s (Figure 2(b)), the peak at $m/z = 300$ shifts to 301, which means that the trap content main constituent is $(C_{24}H_{12}+H)^+$. For increasing irradiation time (Figure 2(c) $t = 2$ s, (d) 3 s, (e) 4 s, and (f) 4.75 s), the peak at $m/z = 301$ disappears progressively while a peak at $m/z = 303$ and then at $m/z = 305$ (for $t = 4.75$ s; see Figure 2(f)) appears, which indicates the addition of three and five hydrogen atoms, respectively. At longer exposure time ($t \sim 15$ s; Figure 3(a)), the $m/z = 303$ peak dominates the signal, and a peak at $m/z = 305$ appears. At even longer irradiation times ($t \sim 30$ s; Figure 3(b)), the peak $m/z = 305$ dominates and peaks at $m/z = 307$ and 309 appear. These peaks clearly show the evolution of the hydrogenation states of coronene cations with H irradiation time.

3. ANALYSIS AND DISCUSSION

Our results show that the most important peaks measured in the mass spectrum shift from lower masses to higher masses with increasing H exposure time. In order to follow the evolution of the first hydrogenated state of coronene cation $(C_{24}H_{12}+H)^+$ ($CorH^+$) to the second $(C_{24}H_{12}+2H)^+$ ($CorH_2^+$), third ($CorH_3^+$), and fourth ($CorH_4^+$) hydrogenated states, we use a simple model that describes this evolution:

$$\frac{dn_{CorH^+}}{dt} = -\left(A_2 e^{-\frac{E_2}{k_B T_{gas}}} n_{CorH^+}\right) n_H, \qquad (1)$$

$$\frac{dn_{CorH_2^+}}{dt} = \left(A_2 e^{-\frac{E_2}{k_B T_{gas}}} n_{CorH^+} - A_3 n_{CorH_2^+}\right) n_H, \qquad (2)$$

$$\frac{dn_{CorH_3^+}}{dt} = \left(A_3 n_{CorH_2^+} - A_4 e^{-\frac{E_4}{k_B T_{gas}}} n_{CorH_3^+}\right) n_H, \qquad (3)$$

$$\frac{dn_{CorH_4^+}}{dt} = \left(A_4 e^{-\frac{E_4}{k_B T_{gas}}} n_{CorH_3^+} - A_5 n_{CorH_4^+}\right) n_H. \qquad (4)$$

Hydrogenation of $CorH_{2n+1}^+$ follows an Arrhenius expression where A_{2n+2} is the prefactor and E_{2n+2} is the barrier, while hydrogenation of $CorH_{2n}^+$ follows the same expression with a prefactor A_{2n+1} and no barrier. k_B is the Boltzmann constant and T the temperature of the H beam ($T \sim 25$ meV).
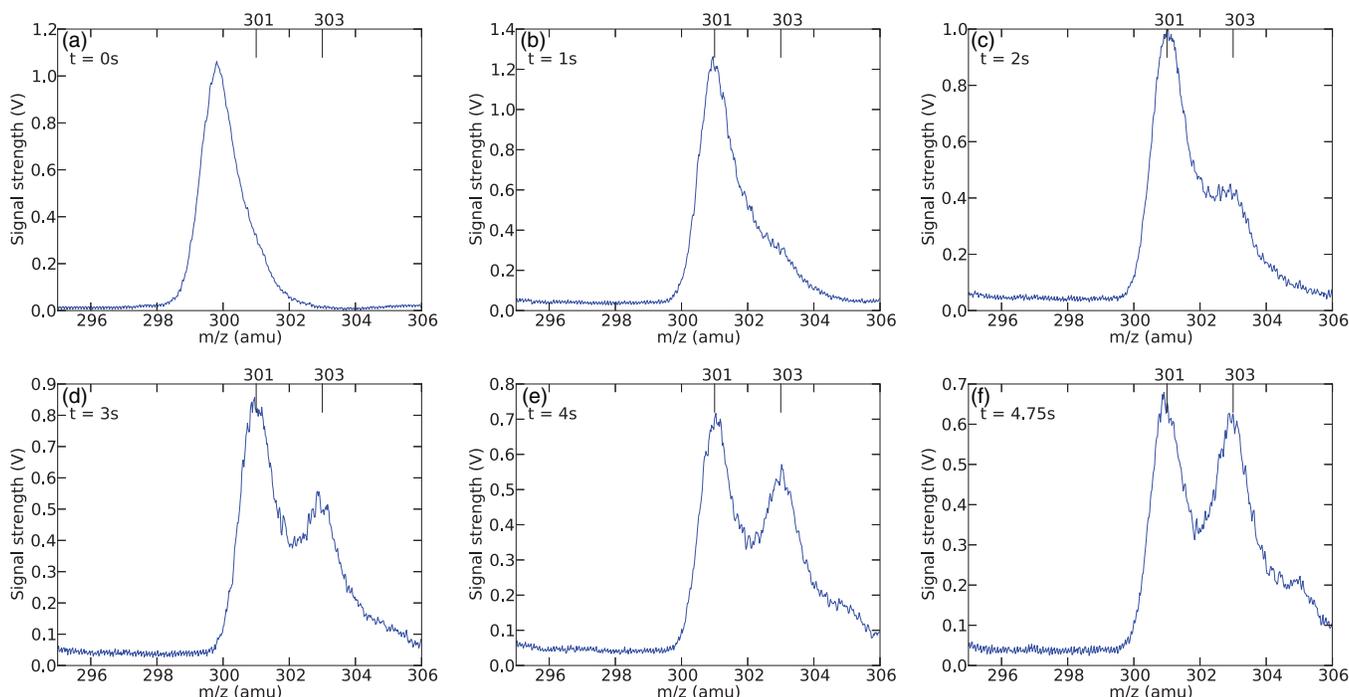
Figure 2. Mass spectrum of coronene (a) without and with exposure to H atoms during (b) 1 s, (c) 2 s, (d) 3 s ,(e) 4 s, and (f) 4.5 s.
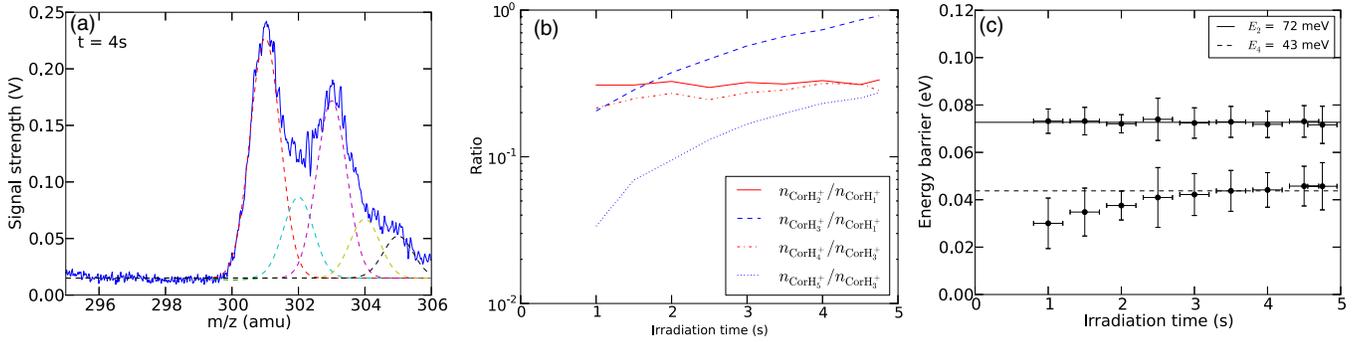(A color version of this figure is available in the online journal.)
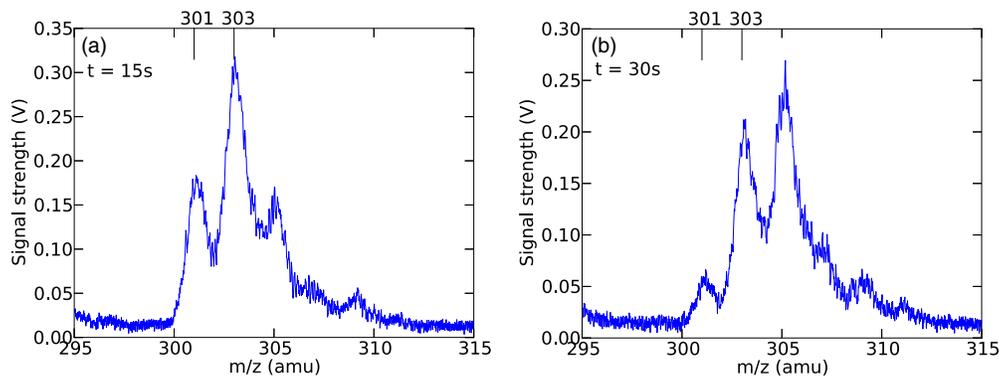
Figure 3. Same as Figure 2 for much longer H exposures of (a) 15 s and (b) 30 s.
(A color version of this figure is available in the online journal.)

In these equations, we do not include abstraction, meaning that the time evolution of the contribution of each state is governed entirely by hydrogenation. This assumption is made in order to derive the first barriers of hydrogenation. Abstraction can be neglected in the conditions of our experiments for low exposure times. This is supported by previous experiments where the cross section for the addition of hydrogen to neutral coronene is predicted to be 20 times that for abstraction (Mennella et al. 2012). Further support is drawn from a kinetic chemical model we developed, which shows that abstraction must be very low compared to hydrogenation to be able to mimic the experimental results (Boschman et al. in prep). However, for long H exposure time we expect the hydrogenation degree of the coronene cations to reach a steady state which will allow us to derive the contribution of abstraction relative to addition, and therefore derive the H_2 formation rate due to PAH cations. It should also be kept in mind that in the conditions of our experiments, the H atoms are at room temperature, meaning that they cross the barriers for abstraction (10 meV; Rauls & Hornekær 2008) and addition (40–60 meV; Rauls & Hornekær

2008) with similar ease. Under interstellar conditions, however, the abstraction will dominate by eight orders of magnitude (at 20 K) because of the barrier differences.

The first hydrogenation is expected to take place at the outer edge carbon atom (Hirama et al. 2004). This state provides more conformational freedom to the four neighboring outer edge carbon atoms, ensuring a preference for the second hydrogenation to take place at one of those four carbon atoms. The third hydrogenation will preferentially take place at the outer edge carbon next to the second H atom. Again, the fourth H atom can be bound to one of the four neighboring outer edge carbon atoms, and the fifth sticks on the neighboring outer edge carbon. This scenario of H atoms sticking preferentially on outer edge carbons next to already adsorbed atoms is described in Rauls & Hornekær (2008).

The contribution of every peak is determined by fitting our data with Gaussians with identical widths (see Figure 4(a)). The ratios between different hydrogenation states as a function of time are reported in Figure 4(b). It appears that the ratio between the contribution of the first (CorH+) and the

Figure 4. (a) Contribution of every peak determined by fitting our data with Gaussians with identical widths. (b) Ratios between different hydrogenation states as a function of time. (c) Barrier heights for the second and fourth hydrogenations.

(A color version of this figure is available in the online journal.)

second ($CorH_2^+$) hydrogenation states does not evolve with time for short timescales (($n_{CorH^+}/n_{CorH_2^+}$) $\sim$ 3 until 5 s). Also, the ratio between the third ($CorH_3^+$) and the forth ($CorH_4^+$) hydrogenation states shows identical behavior after $t \geqslant 2$ s (($n_{CorH_3^+}/n_{CorH_4^+}$) $\sim$ 3 from 2 s onward). Before this exposure time, the $n_{CorH_3^+}$ and $n_{CorH_4^+}$ signals are very weak, and the ratio is uncertain. We can therefore assume that for these measurements $d/dt(n_{CorH_2^+}/n_{CorH^+}) = 0$ and $d/dt(n_{CorH_3^+}/n_{CorH_3^+}) = 0$. The expressions for the $CorH^+$ to $CorH_2^+$ as well as for the $CorH_3^+$ to $CorH_4^+$ energy barriers can then be written as

$$E_2 = -k_B T_{gas} \ln \left(\frac{A_3}{A_2} \frac{1}{1 + \frac{n_{CorH^+}}{n_{CorH_2^+}}} \right) \quad (5)$$

$$E_4 = -k_B T_{gas} \ln \left(\frac{A_5 + A_3 \frac{n_{CorH_2^+}}{n_{CorH_3^+}}}{A_4} \frac{1}{1 + \frac{n_{CorH_3^+}}{n_{CorH_4^+}}} \right). \quad (6)$$

From these expressions, we derive the energy barrier E_2 as 72 ± 6 meV and E_4 as 43 ± 8 meV, as shown in Figure 4(c). This shows that hydrogenation barriers are decreasing with increasing hydrogenation. However, our results also show that odd hydrogenated states dominate the mass spectrum even for high degrees of hydrogenation (Figure 3). This highlights the presence of a barrier–no-barrier alternation from one hydrogenated state to another, up to high hydrogenation states. Our results indicate that even if the hydrogenation barriers decrease for the first hydrogenations, they do not vanish completely and remain at higher hydrogenation states. The barriers derived in our study are similar to the one calculated by Rauls & Hornekær (2008) for neutral coronene. This means that the first hydrogenations of coronene cations should be comparable to the hydrogenation of neutral coronene. However, for a higher degree of hydrogenation we show that these barriers still exist, while the calculations from Rauls & Hornekær (2008) predict that these barriers vanish after a few hydrogenations. Recent mass spectrometric measurements of coronene films exposed to H/D atoms do not show preferences for even or odd hydrogenation states of neutral coronene (Thrower et al. 2012). However, these measurements are not very sensitive to barrier heights well bellow 100 meV, since the experiments were performed with atoms at beam temperature of 170 meV.

In PDRs exposed to UV fields less than few hundreds G_0, the spatial distribution of H_2 and PAHs does correlate (Habart et al. 2003, 2005; Compiègne et al. 2007), contrary to what is seen in the presence of strong UV fields (Tielens et al. 1993; Berné et al. 2009). The H_2 formation rates have been derived

for several PDRs exposed to various UV radiation fields. These rates can be explained by the contribution of PAHs to the formation of H_2 (Habart et al. 2004). Depending on the UV intensity, the PAHs observed can be either PAH cations, which are present in regions at low visual extinctions A_V, or neutral PAHs, which are located at higher extinctions. Wolfire et al. (2008) and Spaans & Meijerink (2005) have shown that high-UV and high-density PDRs ($n_H \geqslant 10^3$ cm^{-3} and $G_0 \geqslant 100$, $G_0 = 1.6 \times 10^{-3}$ erg cm^{-3} s^{-1}) can maintain a $\sim$30% cationic fraction up to a few mag in A_V. More relevant to this work, Cox & Spaans (2006) have studied low-UV PDRs ($G_0 \leqslant 100$), and followed the PAH charge balance for different densities, UV radiation fields, and metallicities. They found that PAH cations dominate over neutrals and anions for $A_V \leqslant 2$ mag. The H_2 formation rates observed in PDRs exposed to different UV fields can therefore be partly attributed to neutral and cationic PAHs.

Our results show that the hydrogenation processes of neutral and cationic PAHs are similar and should contribute similarly to the formation of H_2. Further experimental investigations will allow us to derive the H_2 formation rate for PAH cations.

4. CONCLUSIONS

We have investigated the addition of hydrogen atoms to coronene cations in the gas phase and observed increasing hydrogenation with H exposure time. Our results show that odd hydrogenated states dominate the mass spectrum, which evidences the presence of a barrier for the further hydrogenation of odd hydrogenation states. The first hydrogen sticks to the coronene cations without a barrier (Snow et al. 1998; Hirama et al. 2004). The second and fourth hydrogenations are associated with barriers of about 72 ± 6 meV and 43 ± 8 meV, while the third and fifth hydrogenation are barrierless. These barriers are similar to the one calculated for neutral coronene (Rauls & Hornekær 2008). Our results indicate that superhydrogenated PAH cations (Li & Draine 2012) should also be found in the ISM, and be important catalysts for the formation of H_2, as it is the case for their neutral counterparts.

REFERENCES

Bachellerie, D., Sizun, M., Teillet-Billy, D., Rougeau, N., & Sidis, V. 2007, Chem. Phys. Lett., 448, 223

Bari, S., Gonzalez-Magana, O., Reitsma, G., et al. 2011, J. Chem. Phys., 134, 024314

Bauschlicher, C. W., Jr. 1998, ApJ, 509, L125

Berné, O., Fuente, A., Goicoechea, J. R., et al. 2009, ApJ, 706, L160

Bliek, F., Woestenenk, G., Hoekstra, R., & Morgenstern, R. 1997, Hyperfine Interact., 108, 121

Cazaux, S., Morisset, S., Spaans, M., & Allouche, A. 2011, A&A, 535, A27

Compiègne, M., Abergel, A., Verstraete, L., et al. 2007, A&A, 471, 205

Cox, N. L. J., & Spaans, M. 2006, A&A, 451, 973

Gould, R. J., & Salpeter, E. E. 1963, ApJ, 138, 393

Habart, E., Abergel, A., Walmsley, C. M., Teyssier, D., & Pety, J. 2005, A&A, 437, 177

Habart, E., Boulanger, F., Verstraete, L., Walmsley, C. M., & Pineau des Forêts, G. 2004, A&A, 414, 531

Habart, E., Boulanger, F., Verstraete, L., et al. 2003, A&A, 397, 623

Hirama, M., Tokosumi, T., Ishida, T., & ichi Aihara, J. 2004, Chem. Phys., 305, 307

Hoekstra, R., de Heer, F. J., & Morgenstern, R. 1991, J. Phys. B: At. Mol. Opt. Phys., 24, 4025

Hornekær, L., Rauls, E., Xu, W., et al. 2006, Phys. Rev. Lett., 97, 186102

Le Page, V., Snow, T. P., & Bierbaum, V. M. 2009, ApJ, 704, 274

Li, A., & Draine, B. T. 2012, ApJ, 760, L35

Martinazzo, R., & Tantardini, G. F. 2006, J. Chem. Phys., 124, 124703

Maziarz, E. 2005, Can. J. Chem. (Revue Canadienne de Chimie), 85, 1871

Mennella, V. 2006, ApJ, 647, L49

Mennella, V., Hornekær, L., Thrower, J., & Accolla, M. 2012, ApJ, 745, L2

Morisset, S., Aguillon, F., Sizun, M., & Sidis, V. 2003, Chem. Phys. Lett., 378, 615

Morisset, S., Aguillon, F., Sizun, M., & Sidis, V. 2004, J. Phys. Chem. A, 108, 8571

Oort, J. H., & van de Hulst, H. C. 1946, Bull. Astron. Inst. Netherlands, 10, 187

Perry, J. S. A., & Price, S. D. 2003, Ap&SS, 285, 769

Pirronello, V., Biham, O., Manicó, G., Roser, J. E., & Vidali, G. 2000, in Molecular Hydrogen in Space, ed. F. Combes & G. Pineau Des Forets (Cambridge: Cambridge Univ. Press), 71

Pirronello, V., Liu, C., Roser, J. E., & Vidali, G. 1999, A&A, 344, 681

Pirronello, V., Liu, C., Shen, L., & Vidali, G. 1997, ApJ, 475, L69

Rauls, E., & Hornekær, L. 2008, ApJ, 679, 531

Rougeau, N., Teillet-Billy, D., & Sidis, V. 2006, Chem. Phys. Lett., 431, 135

Sha, X., & Jackson, B. 2002, Surf. Sci., 496, 318

Shah, M. B., & Gilbody, H. B. 1978, J. Phys. B: At. Mol. Phys., 11, 121

Snow, T. P., Le Page, V., Keheyan, Y., & Bierbaum, V. M. 1998, Nature, 391, 259

Spaans, M., & Meijerink, R. 2005, Ap&SS, 295, 239

Spaans, M., & Silk, J. 2000, ApJ, 538, 115

Thrower, J. D., Jørgensen, B., Friis, E. E., et al. 2012, ApJ, 752, 3

Tielens, A. G. G. M., Meixner, M. M., van der Werf, P. P., et al. 1993, Science, 262, 86

Weingartner, J. C., & Draine, B. T. 2001, ApJ, 548, 296

Wolfire, M. G., Tielens, A. G. G. M., Hollenbach, D., & Kaufman, M. J. 2008, ApJ, 680, 384

Zecho, T., Guttler, A., Sha, X., Jackson, B., & Kuppers, J. 2002, J. Chem. Phys., 117, 8486